

# Selective Reduction of Nitroarenes to Arylamines by the Cooperative Action of Methylhydrazine and a Tris(*N*-heterocyclic thioamidate) Cobalt(III) Complex

Dimitris I. Ioannou, Dimitra K. Gioftsidou, Vasiliki E. Tsina, Michael G. Kallitsakis, Antonios G. Hatzidimitriou, Michael A. Terzidis, Panagiotis A. Angaridis,\* and Ioannis N. Lykakis\*

Cite This: *J. Org. Chem.* 2021, 86, 2895–2906

Read Online

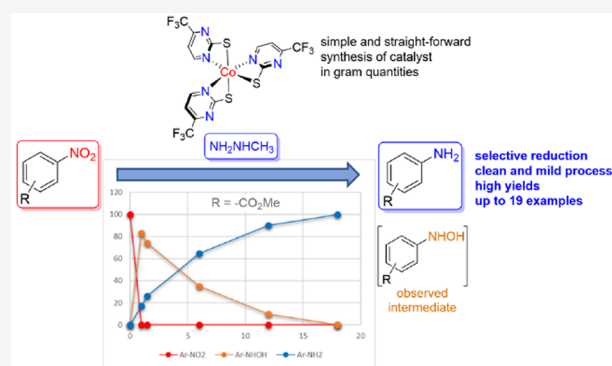
ACCESS |

Metrics & More

Article Recommendations

Supporting Information

**ABSTRACT:** We report an efficient catalytic protocol that chemoselectively reduces nitroarenes to arylamines, by using methylhydrazine as a reducing agent in combination with the easily synthesized and robust catalyst tris(*N*-heterocyclic thioamidate) Co(III) complex  $[\text{Co}(\kappa\text{S},\text{N}\text{-tfmp}2\text{S})_3]$ , tfmp2S = 4-(trifluoromethyl)-pyrimidine-2-thiolate. A series of arylamines and heterocyclic amines were formed in excellent yields and chemoselectivity. High conversion yields of nitroarenes into the corresponding amines were observed by using polar protic solvents, such as MeOH and *i*PrOH. Among several hydrogen donors that were examined, methylhydrazine demonstrated the best performance. Preliminary mechanistic investigations, supported by UV–vis and NMR spectroscopy, cyclic voltammetry, and high-resolution mass spectrometry, suggest a cooperative action of methylhydrazine and  $[\text{Co}(\kappa\text{S},\text{N}\text{-tfmp}2\text{S})_3]$  via a coordination activation pathway that leads to the formation of a reduced cobalt species, responsible for the catalytic transformation. In general, the corresponding *N*-arylhydroxylamines were identified as the sole intermediates. Nevertheless, the corresponding nitrosoarenes can also be formed as intermediates, which, however, are rapidly transformed into the desired arylamines in the presence of methylhydrazine through a noncatalytic path. On the basis of the observed high chemoselectivity and yields, and the fast and clean reaction processes, the present catalytic system  $[\text{Co}(\kappa\text{S},\text{N}\text{-tfmp}2\text{S})_3]/\text{MeNHNH}_2$  shows promise for the efficient synthesis of aromatic amines that could find various industrial applications.



## INTRODUCTION

The selective reduction of a nitro group to an amino group in a compound is a transformation of continuous interest, as the amines serve as intermediates for the production of various pharmaceutical molecules and rubber materials. The simplest process to accomplish this transformation is via transition-metal-catalyzed hydrogenation.<sup>1</sup> The reduction of nitroarenes to anilines<sup>1</sup> often suffers from low chemoselectivity when other reducible functionalities are present; nevertheless, it continues to magnetize the scientific and industrial interest. During the past decade, cobalt catalysts have been successfully used in the reducing transformation of nitroarenes into the corresponding arylamines under hydrogenation or transfer hydrogenation conditions.<sup>2</sup> For the transfer hydrogenation process, among the used hydrogen donor molecules, i.e., borohydrides, hydrosilanes, formic acid, and CO/H<sub>2</sub>O mixture,<sup>2</sup> hydrazine hydrate is reported as the most studied H-donor both in organic and aqueous media.<sup>3–13</sup> Recently, the use of cobalt oxides with hydrazine hydrate under heterogeneous photocatalytic conditions has also been reported.<sup>14</sup>

Except for the most used heterogeneous cobalt nanocatalysts (Scheme 1A), examples incorporating cobalt-based coordina-

tion compounds for the selective reduction of nitroarenes to arylamines under homogeneous conditions are limited. Specifically, catalytically active systems that involve phthalocyanine Co(II) complexes,<sup>9,10</sup> trinuclear mixed valent Co(II)/Co(III)/Co(II) complexes,<sup>11</sup> or Co(II) complexes of pyrrole carboxamide ligands,<sup>12</sup> in combination with hydrazine hydrate as a reducing agent, have been reported so far in the literature (Scheme 1B).<sup>12</sup> Despite different Co(II) complexes used for such reduction process, the development of highly active, selective, easily accessible, and stable Co(III)-based homogeneous catalytic systems remains a challenging task.

Taking all of the above into account, and following our interest in this kind of reductive transformation,<sup>15</sup> we report herein a new and efficient catalytic protocol that accomplishes

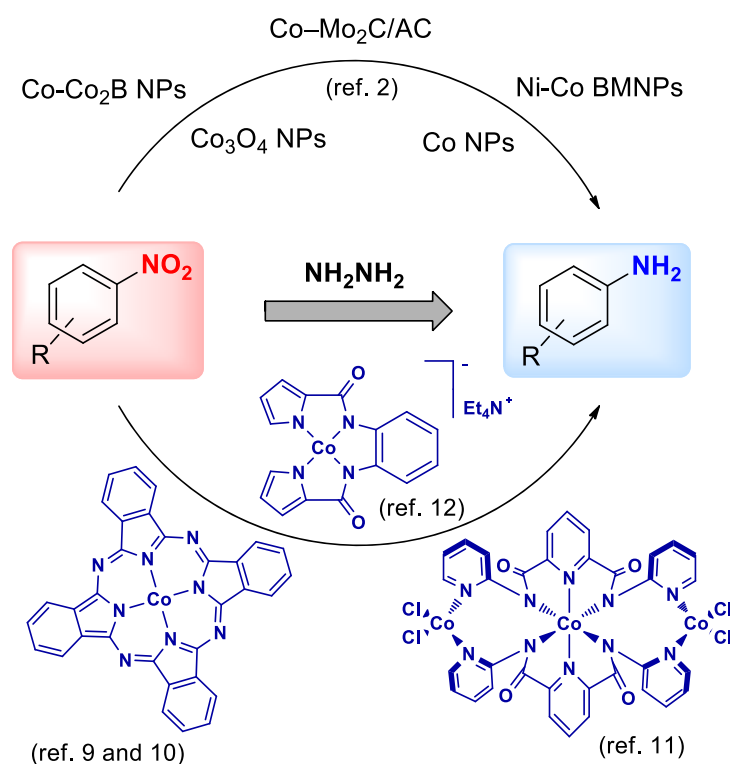
Received: November 25, 2020

Published: January 26, 2021

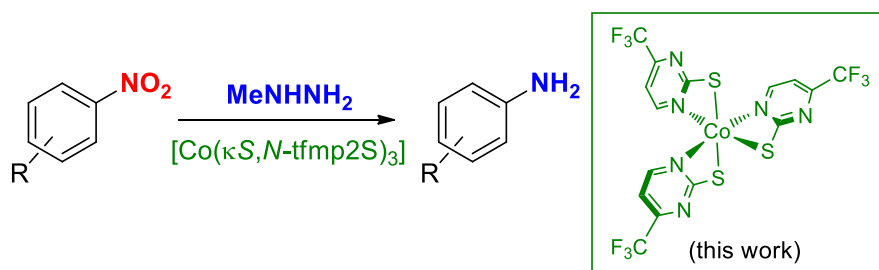


Scheme 1. Hydrazine-Mediated Cobalt-Catalyzed Nitroarene Reductions in Heterogeneous and Homogeneous Processes

### A. Cobalt-nanocatalysts/hydrazine catalyzed processes



### B. Cobalt-complexes/hydrazine catalyzed processes



### C. Co(III)-complexes/methylhydrazine cooperative catalyzed process

the reduction of nitroarenes to arylamines by the combined action of an easily synthesized and robust Co(III) complex that bears three chelating *N*-heterocyclic thioamidate ligands,  $[\text{Co}(\kappa\text{S}, \text{N-tfmp}2\text{S})_3]$ , and methylhydrazine (Scheme 1C). To the best of our knowledge, methylhydrazine is still an unexplored reducing agent in cobalt-catalyzed nitroarene reactions.<sup>2</sup> Furthermore, *N*-heterocyclic thioamidates as ligands of transition-metal complexes, except the fact that they are commercially available reagents, they also offer the possibility of facile control of their stereochemical and electrochemical properties, which, in combination with their hemilability and versatile coordinating ability, renders them ideal candidates for the synthesis of stable, robust, and catalytically active cobalt complexes.<sup>16</sup>

## RESULTS AND DISCUSSION

**Synthesis and Structure of the Catalyst C1.** The homoleptic, tris-chelating *N*-heterocyclic thioamidate Co(III) complex  $[\text{Co}(\kappa\text{S}, \text{N-tfmp}2\text{S})_3]$  (C1) (tfmp2S = 4-(trifluoromethyl)-pyrimidine-2-thiolate) was chosen as a potential catalyst for the conversion of nitroarenes to anilines, owing to the hemilability and versatile coordination ability of its ligands, easy access to the Co(III)/Co(II) redox shuttle, as well as its simplicity, robustness, and its facile synthesis. Indeed, C1 was synthesized in a simple and straightforward manner, from the reaction of  $\text{CoCl}_2 \cdot 6\text{H}_2\text{O}$  with 3 equiv of tfmp2SH, in the presence of an excess of  $\text{Et}_2\text{NH}$ , in MeOH under reflux conditions in air, and isolated as a dark brown solid. Recrystallization from  $\text{CH}_2\text{Cl}_2$ /hexane afforded the product

of the reaction in high purity and high yield (ca. 70%) and, more specifically, in the form of single crystals suitable for X-ray diffraction analysis (crystal structure details and pertinent geometrical parameters of  $\text{C1} \cdot 0.16\text{CH}_2\text{Cl}_2$  are provided in Table S1).<sup>17</sup> As shown in Figure 1, the complex consists of a

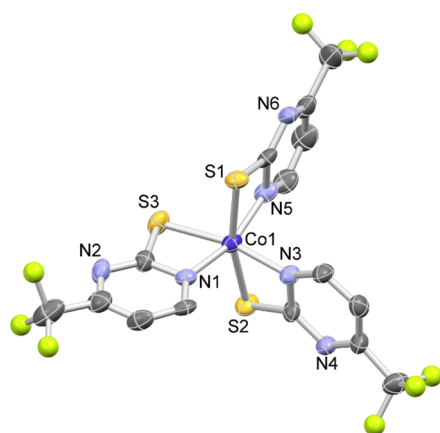


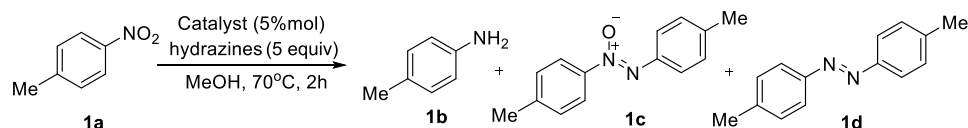
**Figure 1.** View of the molecular structure of  $[\text{Co}(\kappa\text{S},\text{N}\text{-tfmp}2\text{S})_3]$  (**C1**) (only one of the three symmetry independent molecules of the asymmetric unit of the crystal structure is shown). Thermal ellipsoids are shown at the 35% probability level. Hydrogen atoms are omitted for clarity. Color code: Co, purple; S, yellow; N, blue; C, dark gray; F, green.

Co(III) ion surrounded by three *N*-heterocyclic thioamidate anions,  $\text{tfmp}2\text{S}^-$ , bound through their exocyclic S and heterocyclic N donor atoms in a chelating mode, resulting in a distorted octahedral  $\text{N}_3\text{S}_3$  coordination environment. The

major cause for these geometric distortions is the small chelate ring angles formed by the metal center and the donor atoms of the  $\text{tfmp}2\text{S}$  ligands, attributed to their narrow bite angles (the sensitivity of these bond angles to crystal packing forces should also not be neglected, too). The Co–N and Co–S bond lengths fall in the ranges of 1.90–1.94 Å and 2.25–2.31 Å, respectively (see Table S2), which are indicative of low spin, octahedrally coordinated  $d^6$  Co(III) ions. The relative disposition of the three *N*-heterocyclic thioamidate ligands results in a meridional arrangement of the S and N donor atoms around the metal center, which is not unusual for analogous homoleptic *N*-heterocyclic thioamidate Co(III) complexes reported in the literature.<sup>18</sup> The molecular structure of **C1**, as well as its stability in solution, with respect to the relative disposition of the N and S donor atoms, was also verified by  $^1\text{H}$  and  $^{13}\text{C}\{\text{H}\}$  NMR spectroscopy.

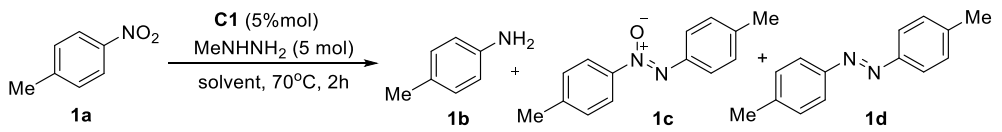
**Catalytic Conditions Evaluation.** The present catalytic protocol arose during the study of the title reaction using 4-nitrotoluene (**1a**) and methylhydrazine in the presence of **C1**. Specifically, **1a** (0.2 mmol) was placed into a 5 mL glass sealed tube together with 1 mL of MeOH and 0.01 mmol of **C1**. Initially, the mixture was magnetically stirred at room temperature for homogenization. Then the appropriate amount of methylhydrazine was added, the tube was sealed, and the reaction mixture was stirred for 2 h at 70 °C (Table 1). Complex **C1** was found to catalyze the reduction process efficiently, resulting in the quantitative formation of the *p*-toluidine (**1b**), in the presence of 5 equiv of methylhydrazine and within 2 h (Table 1, entry 1). It is worth noting that hydrazine hydrate, maybe the most common reducing agent used in the literature in combination with cobalt-based catalysts,<sup>2</sup> under the same reaction conditions led to a lower

**Table 1.** Conditions Evaluation of Hydrazine Mediated Reduction of **1a** to **1b**



entry	catalyst/hydrazines <sup>a</sup>	<b>1a</b> (%) <sup>b</sup>	<b>1b</b> (%) <sup>b</sup>	<b>1c</b> (%) <sup>b</sup>	<b>1d</b> (%) <sup>b</sup>
1	<b>C1</b> /MeNHNH <sub>2</sub>		>99		
2	<b>C1</b> /NH <sub>2</sub> NH <sub>2</sub> ·H <sub>2</sub> O	70	30		
3	<b>C1</b> /Me <sub>2</sub> NNH <sub>2</sub>	100			
4	<b>C1</b> /TsNHNH <sub>2</sub>	100			
5	<b>C1</b> /PhNHNH <sub>2</sub>	64	22	14	
6	<b>C1</b> /MeNHNH <sub>2</sub> (25 °C)	100			
7 <sup>c</sup>	<b>C1</b> /MeNHNH <sub>2</sub> (MW, 20 min)		>99		
8 <sup>d</sup>	<b>C1</b> (2 mol %)/MeNHNH <sub>2</sub>		>99		
9 <sup>e</sup>	<b>C1</b> (1 mol %)/MeNHNH <sub>2</sub>		>99		
10 <sup>f</sup>	<b>C1</b> /MeNHNH <sub>2</sub> (3 equiv)	43	45	4	
11	<b>C1</b> /MeNHNH <sub>2</sub> (3 equiv, 5 h)	29	58	13	
12	<b>C1</b> /MeNHNH <sub>2</sub> (4 equiv, 5 h)		88	12	
13	no catalyst/MeNHNH <sub>2</sub>	100			
14	<b>C1</b> /no MeNHNH <sub>2</sub>	100			
15	[Co(acac) <sub>3</sub> ]/MeNHNH <sub>2</sub>	70	30		
16	[Co(acac) <sub>2</sub> ]/MeNHNH <sub>2</sub>	25	50	10	15
17	Co(NO <sub>3</sub> ) <sub>2</sub> /MeNHNH <sub>2</sub>	32	45	9	14
18	Co(OAc) <sub>2</sub> /MeNHNH <sub>2</sub>	40	60		
19	CoCl <sub>2</sub> /MeNHNH <sub>2</sub>	22	59	12	7

<sup>a</sup>Reaction conditions: **1a** (0.2 mmol), hydrazines (1 mmol), catalyst (5 mol %), in MeOH 1 mL, at 70 °C and for 2 h in a 5 mL sealed tube. <sup>b</sup>Yields based on  $^1\text{H}$  NMR analysis from the integration of the corresponding diagnostic protons of products **1b**, **1c**, and **1d**. <sup>c</sup>70 °C,  $t = 20$  min. <sup>d</sup> $t = 5$  h. <sup>e</sup> $t = 10$  h. <sup>f</sup>The corresponding *N*-(*p*-tolyl)hydroxylamine (**1e**) was formed in 8% relative yield, as determined by  $^1\text{H}$  NMR.

Table 2. Solvent Evaluation in the Reduction of **1a** Catalyzed by **C1**/MeNHNH<sub>2</sub>


entry	solvent <sup>a</sup>	<b>1a</b> (%) <sup>b</sup>	<b>1b</b> (%) <sup>b</sup>	<b>1c</b> (%) <sup>b</sup>	<b>1d</b> (%) <sup>b</sup>
1	MeOH		100		
2	<i>i</i> PrOH		100		
3	EtOH	36	65	9	
4	CF <sub>3</sub> CH <sub>2</sub> OH	29	60	11	
5	H <sub>2</sub> O	100			
6	MeCN	100			
7	DMC	100			
8	DEC	100			
9	1,2-DCE	100			
10	THF	100			
11	THF/H <sub>2</sub> O (9:1)	18	64	12	16
12	THF/MeOH (9:1)	100			
13 <sup>c</sup>	MeCN/MeOH (9:1)	26	27		
14	MeCN/H <sub>2</sub> O (9:1)	48	25	27	

<sup>a</sup>Reaction conditions: **1a** (0.2 mmol), methylhydrazine (1 mmol), **C1** (5% mol), in various solvents, at 70 °C and for 2 h in a 5 mL sealed tube.

<sup>b</sup>Yields are based on <sup>1</sup>H NMR analysis from the integration of the corresponding diagnostic protons. <sup>c</sup>The corresponding *N*-arylhydroxylamine (**1e**) was observed in a 47% relative yield.

reaction conversion of 30% (Table 1, entry 2). No reduction was observed by the utilization of 1,1-dimethylhydrazine (Me<sub>2</sub>NNH<sub>2</sub>) or tosylhydrazine (TsNHNH<sub>2</sub>) (Table 1, entries 3 and 4), although phenylhydrazine (PhNHNH<sub>2</sub>) afforded the desired product at a lower relative yield (22%) along with the corresponding azoxyarene **1b** in 14% yield, as a byproduct (Table 1, entry 5). When the reaction was performed at room temperature in the presence of 5 mol % **C1** and 5 equiv of MeNHNH<sub>2</sub>, **1a** was found to remain intact (Table 1, entry 6). However, when the reaction was performed, under microwave irradiation (MeOH, 70 °C), aniline **1b** was observed as the sole product within only 20 min (Table 1, entry 7). When **C1** loading was reduced to 2 mol %, the reaction completion was observed within 5 h (Table 1, entry 8), while, by lowering even more to 1 mol %, the conversion was almost quantitative within 10 h (Table 1, entry 9). By reducing the amount of methylhydrazine (3 equiv), no reaction completion was observed within 2 h (57% conversion of **1a**), although arylamine **1b** was formed as the major product (44%), accompanying with a small amount of the corresponding azoxyarene (**1c**) (Table 1, entry 10). The corresponding *N*-(*p*-tolyl)hydroxylamine (**1e**) was also formed in 8% yield, as determined by <sup>1</sup>H NMR of the crude reaction mixture after simple filtration over a short pad of silica. However, after the prolonged time (ca. 5 h) and in the presence of 3 equiv of MeNHNH<sub>2</sub>, no reaction completion was observed by <sup>1</sup>H NMR (19% of the remaining **1a**), and the desired aniline **1b** was formed in a 68% yield along with a 13% of the corresponding azoxyarene **1c** (Table 1, entry 11). In addition, using 4 equiv of MeNHNH<sub>2</sub>, the corresponding aniline **1b** was formed in 88% yield accompanying with 12% of the **1c** (Table 1, entry 12). In the absence of either a catalyst or methylhydrazine, under the same experimental conditions, only the starting nitroarene **1a** was observed in the reaction mixture (Table 1, entries 13 and 14), results that confirm the catalytic nature of the described transformation. It is worth noting that the utilization of [Co(acac)<sub>3</sub>] resulted only in the partial conversion of the **1a** to **1b** (Table 1, entry 15);

however; [Co(acac)<sub>2</sub>] leads to a mixture of amine **1b** and the dimers **1c** and **1d** (Table 1, entry 16). Similar results were also obtained, using cobalt salts, i.e., Co(NO<sub>3</sub>)<sub>2</sub>, Co(OAc)<sub>2</sub>, and CoCl<sub>2</sub> in the presence of MeNHNH<sub>2</sub> (Table 1, entries 17–19).

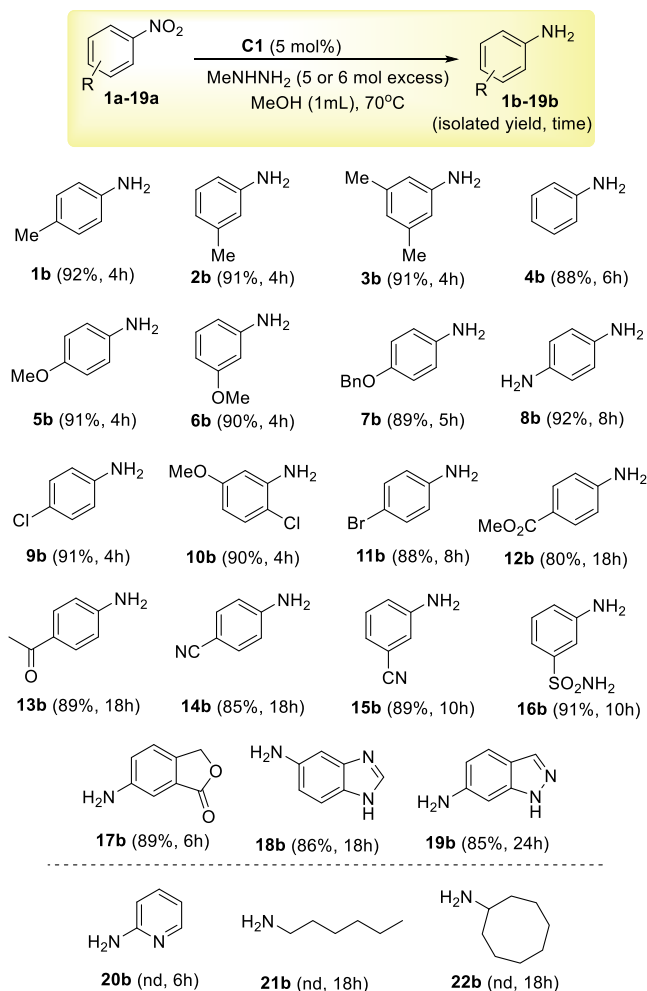
The utilization of other types of hydrogen donor agents, and specifically the 1,1,3,3-tetramethyldisiloxane (TMDS), triethylsilane (Et<sub>3</sub>SiH), dimethylphenylsilane (PhMe<sub>2</sub>SiH), ammonium formate (HCOONH<sub>4</sub>) or formic acid and triethylamine (HCOOH-Et<sub>3</sub>N), or ammonia-borane complex (H<sub>3</sub>N-BH<sub>3</sub>), was found not to promote the desired catalytic transformation (Table S3). Finally, under the same reaction conditions, sodium borohydride (NaBH<sub>4</sub>) afforded an equimolar amount of the desired amine **1b** along with the azoxyarene **1c** (42% and 44%, respectively), as evidenced by <sup>1</sup>H NMR monitoring of the crude reaction mixture (Table S3). All of the above results indicate cooperation between complex **C1** and methylhydrazine, acting as an efficient catalytic system for the selective reduction of nitro compound **1a** to the corresponding amine **1b**.

For us to gain a better understanding of this catalytic transformation, the catalytic efficiency of **C1** was subjected to a solvent screening (Table 2). Among the solvents studied, a high conversion of **1a** was observed by using MeOH and *i*PrOH, followed by EtOH and CF<sub>3</sub>CH<sub>2</sub>OH (Table 2, entries 1–4); however, in water, no reaction process was observed (Table 2, entry 5). In addition, in aprotic polar solvents, CH<sub>3</sub>CN, 1,2-dichloroethane (1,2-DCE), dimethyl carbonate (DMC), diethyl carbonate (DEC), or THF, the reaction did not proceed (Table 2, entries 6–10). The solvent system THF/H<sub>2</sub>O (9:1) that is commonly used in similar transformations underperformed under these conditions (Table 2, entry 11). Similar results were observed when polar solvents, methanol or water, were used in a ratio of 1:9 with THF or MeCN (Table 2, entries 12–14).

After establishing the optimal reaction conditions, we investigated the broadness of the application of the described catalytic procedure toward various nitroarenes. Interestingly,

this catalytic procedure shows a broad functional group tolerance and a series of nitroarenes (**1a–19a**) reduced selectively into the corresponding arylamines (**1b–19b**) in high yields after product isolation (85–92%) and excellent selectivity (>99%), as depicted in Scheme 2. In all cases,

**Scheme 2. Selective Reduction of Nitroarenes 1a–22a Catalyzed by C1 in the Presence of Methylhydrazine**

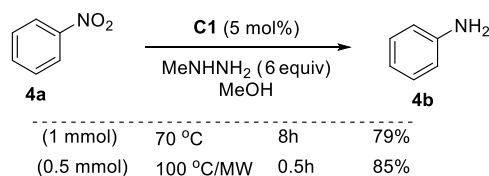


almost quantitative consumption of the starting nitroarene (>98%) was observed by the <sup>1</sup>H NMR spectra of the crude reaction mixture at appropriate reaction times reported in parentheses below each substrate in Scheme 2. Notably, nitroarenes substituted with electron-donating groups, MeO, BnO, and NH<sub>2</sub> (**2a**, **3a**, **5a–8a**), reacted at higher rates and gave better yields when compared with nitroarenes bearing electron-withdrawing substituents, i.e., carboxylate, carbonyl, cyano-, and sulfonamide (**12a–16a**), which required a higher mol excess of methylhydrazine (6 equiv instead of 5 equiv) and prolonged reaction times. Importantly, chloro- and bromo-substituted nitroarenes (**9a–11a**) were reduced without undergoing any reductive dehalogenation, and the corresponding halogenated-substituted anilines **9b–11b** were formed in high isolated yields (88–91%, Scheme 2). In addition, carbonyl and cyano functionalities in nitroarenes (**13a–15a**) remained intact, indicative of a highly chemoselective process. In the case of 4-nitrophenylethanone (**13a**), the corresponding 4-aminophenylethanone (**13b**) was isolated in 89% yield

without the isolation of the corresponding 4-nitrophenyl ethyl methylhydrazone, from the reaction between the methylhydrazine and the carbonyl compound. Due to the simplicity of the present catalytic protocol, we also attempted the reduction of different heterocyclic nitro compounds (**17a–19a**), where the corresponding amines (**17b–19b**) were isolated in high yields, 85–89% (Scheme 2). The reactions for compounds **20a–22a** were also performed under the same experimental conditions but also for a prolonged reaction time (18 h). Unexpectedly, 2-nitropyridine (**20a**) showed poor reactivity, while the aliphatic nitroalkanes **21a** and **22a** gave a mixture of unidentified products in ca. 10–15% conversion. However, in all cases, the corresponding amines were not observed based on the <sup>1</sup>H NMR spectra of the crude reaction mixtures (Scheme 2, nd = not detected).

To assess the scalability potential of this process, the reduction of **4a** was also carried out at a 1 mmol scale, with 5% mol of **C1**, 6 mmol of methylhydrazine, and 7 mL of MeOH at 70 °C in a 15 mL sealed tube. After reaction completion (8 h), monitored by TLC, the solvent was removed under reduced pressure, and the reaction mixture was filtered over a short path of Celite and silica gel with the assistance of ethyl acetate (~15 mL) for separating the catalyst from the reaction mixture. After solvent evaporation under reduced pressure, the residue was purified with column chromatography, and the corresponding amine **4b** was isolated in 79% yield. For comparison reasons, a 0.5 mmol reaction scale under MW conditions at 100 °C gave **4b** in 85% isolated yield within 30 min, a result that supports further the potential use of the present methodology in synthetic applications (Scheme 3).

**Scheme 3. Lab-Scale Synthesis of 4b in the Presence of the C1/Methylhydrazine Catalytic System**



**Mechanistic Studies.** An explanation of the catalytic efficiency of **C1** might be provided by considering the properties of its ligands. The relatively low stability of the four-membered chelate rings of its *N*-heterocyclic thioamidate ligands and the weak Lewis base character of the ttmp2S moieties contribute to their hemilability on the metal center. Based on this fact, and in combination with their ability to easily adopt different coordination modes (either monodentate or bidentate), it is highly possible that they are amenable to easily open a coordination site on the metal center to facilitate the subsequent attachment of methylhydrazine or substrate. An analogous mechanism of action for heterocyclic thioamidates has been proposed in the literature for analogous tris(*N*-heterocyclic thioamidate) Ni(II) complexes that have been utilized in the photocatalytic reduction of H<sup>+</sup> to H<sub>2</sub>.<sup>19</sup>

(i) To get an insight into the mechanism of the reaction and, in particular, the synergy between **C1** and methylhydrazine,<sup>20</sup> cyclic voltammetry (CV), UV–vis spectroscopy, and high-resolution mass spectrometry (HRMS) measurements were conducted. The cyclic voltammogram of **C1** in MeOH displays a nearly reversible redox process with  $E_{1/2} = -0.714$  V ( $\Delta E =$

0.159 V) vs Fc/Fc<sup>+</sup> (Figure 2, black line), which can be assigned to the Co(III)/Co(II) redox couple. The

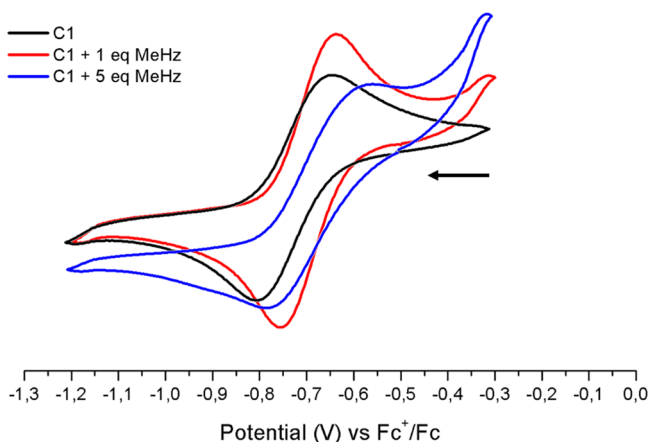


**Figure 2.** Cyclic voltammetry data of C1 in MeOH after the addition of 1 and 5 equiv of MeNHNH<sub>2</sub>. Potentials are referenced to  $E_{1/2}(\text{Fc}/\text{Fc}^+) = 0$ .

relatively easily accessible reduction potential of C1 suggests that C1 can be potentially easily reduced by MeNHNH<sub>2</sub> at an initial stage of the reaction. UV–vis spectroscopy measurements provide verification of this assumption. A dark-brown-green solution of C1 in MeOH displays, in the low energy region of 600–700 nm, a characteristic low-intensity absorption band ( $\epsilon = 163 \text{ M}^{-1} \text{ cm}^{-1}$ ), which can be assigned to a d–d electronic transition. However, the addition of 1 equiv of MeNHNH<sub>2</sub> results in a color change to lighter brown and disappearance of this band, a fact that can be attributed to a change in the electronic structure of the

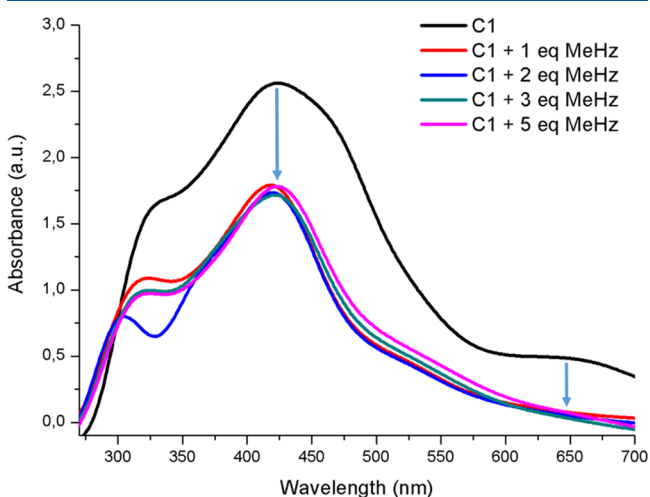


**Figure 3.** UV–vis spectra of C1 in MeOH after addition of 1 to 5 equiv of MeNHNH<sub>2</sub>.

complex, as a result of the reduction to Co(II) (Figure 3).

In the presence of 1 equiv of methylhydrazine, the cyclic voltammogram of C1 (red line, Figure 2) shows a nearly reversible Co(III)/Co(II) redox response, which is shifted to more positive values compared to C1 (black line, Figure 2)

( $-0.697 \text{ V}$ ,  $\Delta E = 0.118 \text{ V}$  vs Fc/Fc<sup>+</sup>). Such a fact suggests that methylhydrazine coordinates to the metal center, and an equilibrium formation of the methylhydrazine adduct is established.<sup>21</sup> The formation of this adduct is supported by HRMS measurements of the 1:1 mixture of C1 with MeNHNH<sub>2</sub> in MeOH and the appearance of a mass peak at  $m/z$  642.9616, which can be assigned to the methylhydrazine coordinated monocationic adduct  $[\text{C1}(\text{CN}_2\text{H}_6)+\text{H}^+]^+$  (Figure S2). The formation of such a methylhydrazine-coordinated cobalt intermediate species may provide a way for methylhydrazine activation, possibly by weakening a N–H bond, enabling H<sub>2</sub> evolution, and leading to the formation of a metal hydride intermediate.<sup>2c</sup> Despite the fact that, over the course of our investigations, we observed the formation of H<sub>2</sub> by thermal conductivity detector gas chromatography (TCD-GC) monitoring of the reaction mixtures,<sup>15g</sup> we were not able to detect any Co-hydride intermediate, e.g., by on-line monitoring the <sup>1</sup>H NMR experiments described below (apparently due to its low stability in the reaction medium).<sup>22</sup> However, the formation of such intermediate species might not be excluded, as described by others in analogous reductive transformations mediated by hydrazine and transition metal complexes.<sup>23</sup>

Further addition of 5 equiv of methylhydrazine in a solution of C1 resulted in the appearance of a new mass peak at  $m/z$  507.0035, which can be assigned to a new monocationic cobalt species formed by the removal of a tfmp2S ligand from C1 and the coordination of a CH<sub>3</sub>NHNH<sub>2</sub> and a CH<sub>2</sub>=NNH<sub>2</sub> (or CH<sub>3</sub>N=NH, diazene), i.e.,  $[(\text{C1-tfmp2S})(\text{CN}_2\text{H}_6)(\text{CN}_2\text{H}_4)]^+$  (Figure S3). The existence of such kind of intermediate species might be responsible for the redox response of C1 with 5 equiv of MeNHNH<sub>2</sub>, which shows a slightly different profile compared to the other two voltammograms, and the Co(III)/Co(II) redox potential is positively shifted with respect to C1 (blue line, Figure 2). An analogous metal-diazene species has been previously reported in the literature for other transition metal complexes.<sup>24</sup> Besides, the formation of CH<sub>2</sub>=NNH<sub>2</sub> has also been detected by <sup>1</sup>H NMR spectroscopy measurements, when 0.02 mmol of methylhydrazine was added into a 0.5 mL CD<sub>3</sub>OD solution containing 0.02 mmol of C1; the mixture was stirred for 1 h and then monitored directly by <sup>1</sup>H NMR (Figure S4), therefore, providing another piece of evidence for the proposed pathway.<sup>25</sup>

Overall, these findings suggest that the formation of a methylhydrazine-coordinated cobalt intermediate species is a crucial step for the catalytic reaction, as it imposes a coordination-induced activation pathway<sup>26</sup> that provides a subsequent electron transfer (ET) between C1 and methylhydrazine, leading to a Co(II) species ( $[\text{Co}]$ ), which takes an active role in the catalytic reaction. Further studies underway in our research groups are focused on a deeper understanding of the mechanism of the catalytic reaction, both by experimental and computational methods, as well as on the study of the effect of metal coordination environment on the catalytic efficiency.

- (ii) The generally accepted reduction scheme of aromatic nitro compounds includes two different pathways:<sup>27</sup> a direct route where the final amine is formed through the formation of the corresponding hydroxylamine and nitroso intermediates and a second condensation route, where the corresponding dimers azoxy-, azo-, and hydrazo-compounds that are initially formed

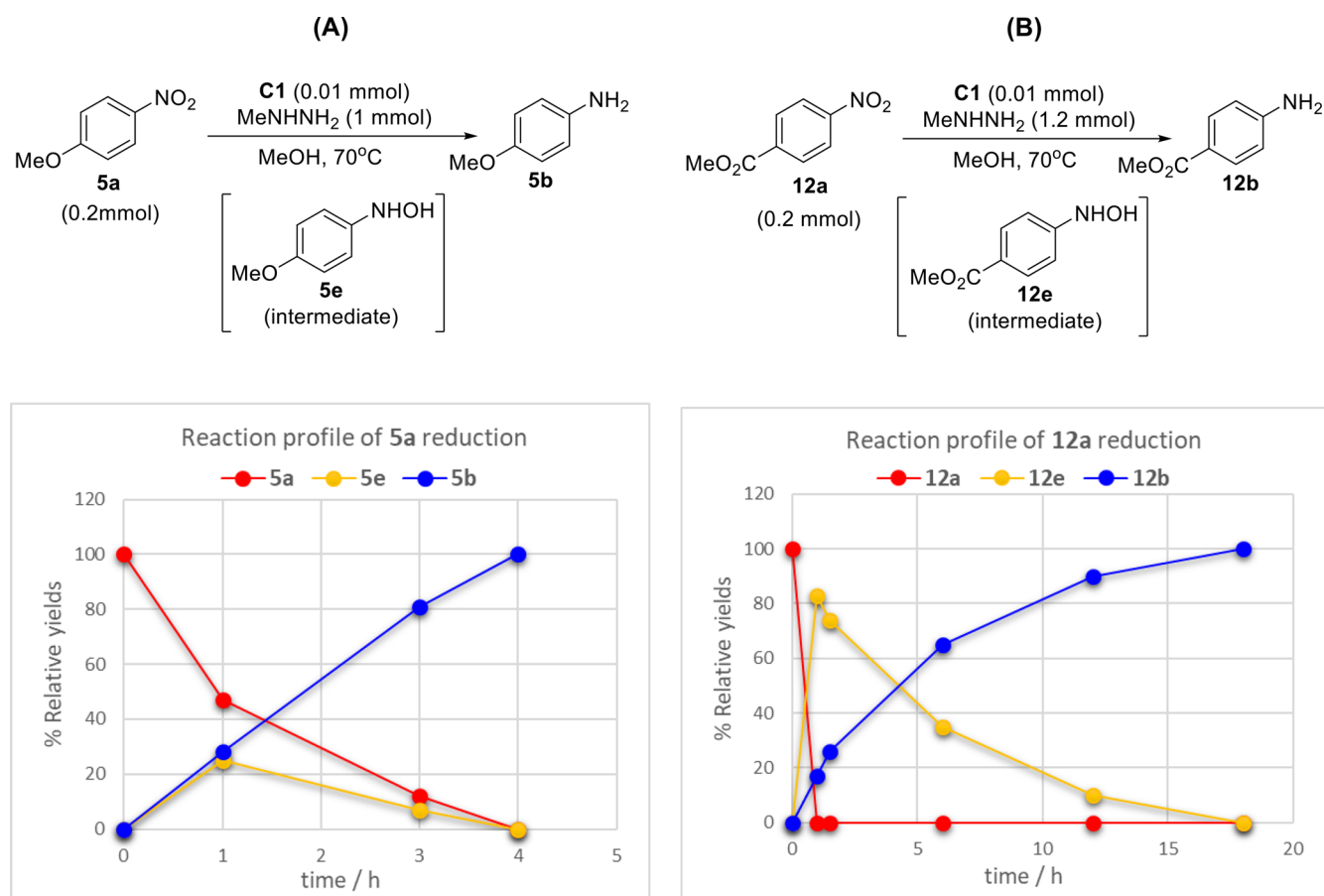


**Figure 4.** Reaction profiles for the reduction of nitroarenes **5a** (A) and **12a** (B) catalyzed by **C1** in the presence of methylhydrazine.

decompose into the final amine. Thus, we initially aimed to determine the reduction pathway occurring herein, by attempting the reduction of the corresponding dimers azoxyarene **1c**, 1,2-diphenylhydrazine **4f**, or hydrazobenzene **4d** under the present conditions. However, no conversion into the corresponding amines **1b** and **4b** was observed, a result that supports a direct route followed by the present reduction process (Figure S5).

Furthermore, experiments were performed in deuterated methanol (CD<sub>3</sub>OD) in order to have a direct reaction monitoring by <sup>1</sup>H NMR. For rich-substituted nitroarene **5a** (4-MeO), the intermediate *N*-arylhydroxylamine (*N*-AHA) **5e** and the product 4-aminoanisole **5b** were observed in almost equal amounts within 1 h (26% and 30%, respectively); however, a significant amount of the starting **5a** (44%) was also presented (Figure S6). On the other hand, in the reduction of the nitroarene **12a** bearing an electron-withdrawing group (4-MeOOC), the corresponding *N*-AHA **12e** was observed in 80% yield, accompanied by the desired arylamine **12b** in 20% yield (Figure S7). Based on these results, it can be proposed that, during the present reduction process, the corresponding *N*-AHA was observed as the only observed intermediate; the result further supports a direct mechanistic route.

(iii) To support the above-mentioned reduction scheme and get a better understanding of the reaction kinetics, a formal reaction profile analysis of the electron-rich (4-MeO, **5a**) and electron-poor (4-Cl, **9a**, 4-CN, **14a**, and 4-MeOOC, **12a**) substituted nitroarenes was performed (Figure S8). At appropriate times, a 100 μL aliquot of

the reaction mixture was taken, and the relative yields of the compounds were determined by <sup>1</sup>H NMR. The reduction kinetics of nitroarenes were found to be heavily affected by the nature of the substituent group (Figure 4). Thus, electron-poor substituted nitroarenes **9a**, **12a**, and **14a** were consumed within a shorter reaction time than the electron-rich substituted nitroarene **5a** (Figure S8). In Figure 4, the reaction profiles for the reduction of nitroarenes **5a** (A) and **12a** (B) were presented. In addition to this result, a formal kinetic analysis was also performed (Figure S9). Assuming a pseudo-first-order dependence of the reaction rate on the nitroarene concentration at a short reaction time (<1 h), eq 1 can be applied:

$$\ln(x) = -kt \quad (1)$$

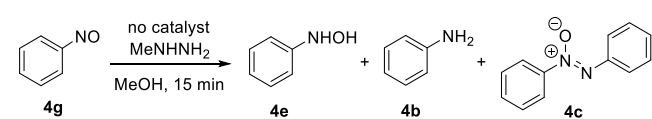
where  $k$  is the rate constant, and  $x$  is the consumption of the *para*-substituted nitroarene at reaction time  $t$ .

According to this equation, a plot of  $-\ln(x)$  versus time should provide a linear curve with a slope equal to the rate constant  $kx$  (Figure S9). Based on these measurements, the reduction rates of **12a** (4-MeOOC) and **14a** (4-CN) were found to be approximately nine and six times faster, respectively, than the corresponding reduction of the **5a** (4-MeO),  $k_{\text{COOMe}}/k_{\text{MeO}} = 9.1$  and  $k_{\text{CN}}/k_{\text{MeO}} = 6.1$  (Figure S9). This result indicates the occurrence of a hydride transfer or a negative charge in the transition state of the nitroarene reduction, which is better stabilized by electron-withdrawing substituents. Similar kinetic results were reported in previous

literature works on the nitroarene reduction using the Au/TiO<sub>2</sub>-hydrazine catalytic system.<sup>15b</sup>

- (iv) Besides the *N*-AHA, which were observed as the only intermediates by <sup>1</sup>H NMR spectroscopy, the formation of the nitrosoarene intermediates cannot be excluded. For example, when nitrosobenzene **4g** reacted with a 5 mol excess of methylhydrazine at the present conditions, within 15 min and in the absence of the catalyst, the corresponding amine **4b** was formed in a high yield (70%), accompanied by the corresponding *N*-phenylhydroxylamine **4e** in a smaller amount (30%) (Table 3,

**Table 3. Reactions of Nitrosobenzene in the Presence of Methylhydrazine in Methanol**



entry	conditions (°C) <sup>a</sup>	MeNHNH <sub>2</sub> (equiv)	4e (%)	4b (%)	4c (%)
1	70	5	30	70	
2	28	5	53	47	
3	28	3	54	42	4
4	28	2	51	38	11

<sup>a</sup>The reactions were performed in 1 mL of MeOH and the relative product yields were determined by <sup>1</sup>H NMR.

entry 1). Of note is that the same noncatalytic reaction proceeds even at a lower temperature, 28 °C, with 5 equiv of methylhydrazine in MeOH, yielding to a mixture of the *N*-arylhydroxylamine **4e** and the amine **4b** in almost equal amounts (Table 3, entry 2), as determined by <sup>1</sup>H NMR. In addition, when a lower amount of methylhydrazine was used (3 or 2 mol excess), *N*-AHA and the amine **4b** were also formed as major products, but also small amounts of azoxybenzene **4c** were observed (Table 3, entries 3 and 4). Therefore,

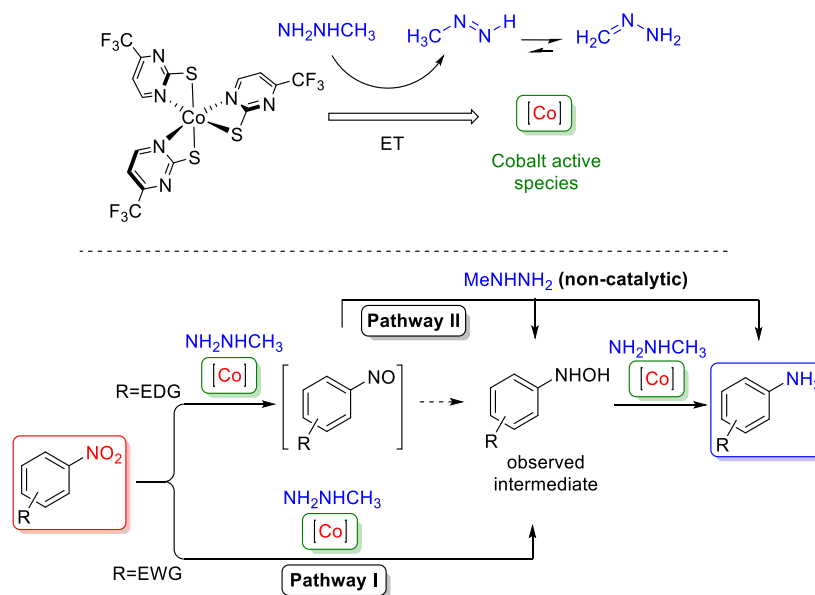
nitrosoarene cannot be excluded as an intermediate in the present catalytic reduction,<sup>28</sup> since it can be fast and directly transformed into the desired aniline through a noncatalytic pathway in the presence of methylhydrazine.

On the basis of the above experimental results, we propose a plausible reduction mechanism that includes two pathways following the direct route shown in Scheme 4. Initially, an ET between methylhydrazine and C1 is taking place, leading to the formation of a reduced Cobalt species [Co], which is responsible for the catalytic reduction pathway. Subsequently, methylhydrazine is transformed into the formyl hydrazone or diazine species. A direct route is proposed, in which the final amine is formed through the formation of the corresponding *N*-AHA, as the only observed intermediate (Pathway I, Scheme 4). The electron poor-substituted nitroarenes are consumed faster than the corresponding rich-substituted nitroarenes, based on kinetic reaction profile experiments. Nitrosobenzene, although not observed under the present reduction processes, is directly reduced into the corresponding aniline in the presence of methylhydrazine via a noncatalytic pathway (Pathway II, Scheme 4). Finally, the observed intermediate *N*-AHA is further reduced to the desired arylamine after the insertion in the catalytic cycle.

## CONCLUSIONS

In conclusion, herein we report the synthesis of a homoleptic tris(*N*-heterocyclic thioamidate) Co(III) complex [Co( $\kappa$ S,*N*-tfmp2S)<sub>3</sub>] and the utilization of such type of compound, for the first time, as a catalyst for the reduction of nitroarenes into the arylamines in the presence of methylhydrazine. The ability of [Co( $\kappa$ S,*N*-tfmp2S)<sub>3</sub>] to catalyze the reaction very efficiently and in a chemoselective manner, under mild and clean reaction conditions, reveals its potential as a simple, robust, and effective catalyst for the particular reaction. A cooperative pathway between the Co(III) complex and methylhydrazine is proposed, based on preliminary experimental data, which support a coordination activation pathway that leads to the

**Scheme 4. Proposed Mechanism for the Reduction of Nitroarenes into Arylamines Catalyzed by [Co( $\kappa$ S,*N*-tfmp2S)<sub>3</sub>]/Methylhydrazine System**



formation of a reduced cobalt species ([Co]) that performs the catalytic reaction. The corresponding *N*-AHA were found to be the sole intermediates. Nevertheless, the corresponding nitrosoarenes could also be formed, which, however, in the presence of methylhydrazine, are rapidly transformed into the arylamines through a noncatalytic path. On the basis of the high chemoselectivity of the reaction, as well as the fast and clean reaction processes, the catalytic system [Co( $\kappa$ S,*N*-tfmp2S)<sub>3</sub>]/MeNHNH<sub>2</sub> presented herein can be used for various hydrogenation reactions, including the fine synthesis of amines.

## EXPERIMENTAL SECTION

**General Procedures and Chemical Reagents.** Solvents and nitroarenes were used without further purification, although the appropriate solvents used for complex C1 synthesis were purified according to established methods and allowed to stand over molecular sieves for 24 h. 4-(Trifluoromethyl)-pyrimidine-2-thiol (tfmp2SH), diethylamine (Et<sub>2</sub>NH), hydrazines, hydrosilanes, nitroarenes, nitrosobenzene, as well as CoCl<sub>2</sub>·6H<sub>2</sub>O, [Co(acac)<sub>3</sub>], [Co(acac)<sub>2</sub>], Co(NO<sub>3</sub>)<sub>2</sub>·6H<sub>2</sub>O and Co(OAc)<sub>2</sub>·4H<sub>2</sub>O were obtained from commercial sources and used without any further purification.

**Instrumentation.** Elemental analyses were obtained on a PerkinElmer 240B elemental microanalyzer. Infrared spectra were recorded on a Nicolet FT-IR 6700 spectrophotometer in the region of 4000–400 cm<sup>-1</sup> as KBr pellets. UV–vis electronic absorption spectra were obtained on a Hitachi U-2001 spectrophotometer. Cyclic voltammetry measurements were carried out on an Autolab electrochemical analyzer, using a platinum working electrode, a platinum counter electrode, and an Ag/AgCl electrode saturated with a KCl reference electrode in 10 mL of MeOH solutions with TBABF<sub>4</sub> as a supporting electrolyte, with a scan rate of 100 mV s<sup>-1</sup>. Product analysis was conducted by <sup>1</sup>H NMR and <sup>13</sup>C{H} NMR spectroscopy (Agilent AM 500 and Agilent AM 600, Agilent Technologies, Santa Clara, CA, USA). Identification of the products was realized by comparing the NMR spectra with those of the commercially available pure substances. An LC–MS 2010 EV instrument (Shimadzu, Tokyo, Japan) under electrospray ionization (ESI) conditions was used for the determination of the mass spectra. The microwave (MW) experiments were performed in a scientific focused MW reactor, Biotage Initiator 2.0, United Kingdom, and online monitoring of the reaction mixture temperature, pressure, and irradiation power was based on the reactor's readings. All of the reagents and solvents were purchased from Sigma-Aldrich, Fluorochem, and Acros and used without further purification. Thin-layer chromatography was performed on Millipore precoated silica gel plates (0.20 mm thick, particle size = 25 μm). Chemical shifts for <sup>1</sup>H NMR were reported as δ values, and coupling constants were measured in hertz (Hz). The following abbreviations were used for spin multiplicity: s = singlet, br s = broad singlet, d = doublet, t = triplet, q = quartet, quin = quintet, dd = double of doublets, ddd = double doublet of doublets, and m = multiplet. Infusion experiments were carried out on an Agilent Q-TOF mass spectrometer, G6540B model with Dual AJS ESI-MS. All of the compounds (dissolved in LC-MS grade, methanol) were introduced into the ESI source of the MS with a single injection of 15 μL of the sample and with a flow rate of 300 μL/min of 100% methanol as a solvent in the binary pump. The experiments were run using a Dual AJS ESI source, operating in a positive ionization mode. Source operating conditions were as follows: 330 °C = gas temp, 8 L/min = gas flow, sheath gas temp = 250 °C, sheath gas flow = 10 L/min, and 150 V = fragmentor. Data-dependent MS/MS analysis was performed in parallel with the MS analysis in a centroid mode, using different collision energies (10, 20, 30, and 40 V). All accurate mass measurements of the [M + H] ions or the corresponding major ions, in some cases, were carried out by scanning from 100 to 1500 *m/z*. The Q-TOF was calibrated 1 h prior to the infusion experiments by using a calibration mixture.

**Single-Crystal X-ray Structure Determinations.** Single-crystal, X-ray diffraction data were collected on a Bruker Apex II CCD area-detector diffractometer, equipped with a Mo Kα (λ = 0.71073 Å) sealed tube source, at 295 K, using the φ and ω scans technique. The program Apex2 (Bruker AXS, 2006) was used in data collection, cell refinement, and data reduction.<sup>29</sup> Structures were solved and refined with full-matrix least-squares using the program Crystals.<sup>30</sup> Anisotropic displacement parameters were applied to all non-hydrogen atoms (except for disordered atoms), while hydrogen atoms were generated geometrically and refined using a riding model. Plots of the molecular structures of all compounds were obtained by using the program Mercury.<sup>31</sup>

**Synthesis of [Co( $\kappa$ -S,*N*-tfmp2S)<sub>3</sub>] (C1).** CoCl<sub>2</sub>·6H<sub>2</sub>O (0.119 g, 0.5 mmol) was dissolved in 15 mL of MeOH. To a 15 mL solution of tfmp2SH (1.5 mmol) in MeOH was added Et<sub>2</sub>NH (1.5 mmol) dropwise. The solution of the heterocyclic thioamide was stirred at room temperature for 30 min, and then, it was transferred to the cobalt-containing solution. The reaction mixture was stirred at 60 °C for 3 h, in air. After filtration, the dark brown filtrate was set aside to evaporate slowly at room temperature, leading, over a period of a few days, to the deposition of a dark brown solid. Recrystallization from CH<sub>2</sub>Cl<sub>2</sub>/hexane resulted in the formation of single crystals of C1·0.16CH<sub>2</sub>Cl<sub>2</sub>. Yield: 0.417 g, 70%. Anal. Calcd for C<sub>15</sub>H<sub>6</sub>CoF<sub>9</sub>N<sub>6</sub>S<sub>3</sub>·0.16CH<sub>2</sub>Cl<sub>2</sub>: C, 29.84; H, 1.05; N, 13.77. Found: C, 30.07; H, 1.26; N, 13.53. FTIR (KBr, cm<sup>-1</sup>): 3415(mbr), 1637(w), 1617(w), 1572(s), 1555(s), 1421(m), 1364(s), 1328(s), 1194(sbr), 1150(sbr), 1112(s), 1018(w), 1010(w), 834(m), 831(m), 736(m), 688(m), 618(wbr), 525(w), 485(w). UV–vis (CH<sub>2</sub>Cl<sub>2</sub>), λ<sub>max</sub>/nm (ε/M<sup>-1</sup> cm<sup>-1</sup>): 269 (40313), 642 (163). <sup>1</sup>H NMR (600 MHz, CDCl<sub>3</sub>): 8.64 (s, 1H), 8.60 (s, 1H), 7.74 (s, 1H), 7.22 (s, 1H), 7.09 (s, 1H), 6.98 (s, 1H). <sup>13</sup>C{H} NMR (151 MHz, CDCl<sub>3</sub>): 187.3, 185.6, 185.0, 161.0, 159.9, 158.0 (q, <sup>2</sup>J<sub>C-F</sub> = 36.4 Hz), 157.8, 157.5 (q, <sup>2</sup>J<sub>C-F</sub> = 36.4 Hz), 157.1 (q, <sup>2</sup>J<sub>C-F</sub> = 36.5 Hz), 119.09 (q, <sup>1</sup>J<sub>C-F</sub> = 276.9 Hz), 119.06 (q, <sup>1</sup>J<sub>C-F</sub> = 276.9 Hz), 119.0 (q, <sup>1</sup>J<sub>C-F</sub> = 277.1 Hz), 111.0 (q, <sup>3</sup>J<sub>C-F</sub> = 2.1 Hz), 110.7 (q, <sup>3</sup>J<sub>C-F</sub> = 2.2 Hz), 109.9 (q, <sup>3</sup>J<sub>C-F</sub> = 2.1 Hz).

**General Catalytic Reduction.** To a sealed tube containing the nitro compound (0.2 mmol) and 1 mL of methanol were added 1 or 1.2 mmol of MeNHNH<sub>2</sub> and the cobalt(III) catalyst C1 (5% mol). The reaction was heated at 70 °C with the use of an oil bath for an appropriate time. The reaction was monitored by TLC, and after completion, the slurry was filtered under reduced pressure through a short pad of silica gel to withhold the catalyst with the aid of ethyl acetate that was also used as a washing solvent for the filter cake. The filtrates and washings were pooled and then evaporated under a vacuum to afford the corresponding amines in pure form. In the case of further purification with column chromatography using silica gel, a gradient mixture of hexane–EtOAc was used as described in detail in each product below. The spectroscopic data (<sup>1</sup>H NMR, <sup>13</sup>C{H} NMR) of amines (**1b**–**19b**) are in agreement with those previously reported.

**Lab-Scale Catalytic Reduction.** To a 15 mL sealed tube containing the nitro compound **4a** (1 mmol) and 7 mL methanol were added 6 mmol of MeNHNH<sub>2</sub> and the cobalt(III) catalyst C1 (5% mol). The reaction was heated to 70 °C with the use of an aluminum heating block for an appropriate time and was monitored by TLC; after completion (8 h), the slurry was filtered under reduced pressure through a short pad of silica gel to withhold the catalyst with the aid of ethyl acetate (~15 mL) for separating the catalyst from the reaction mixture. After solvent evaporation under a vacuum, the residue was purified with column chromatography using a gradient mixture of hexane–EtOAc (10:1 to 1:5), and the corresponding amine **4b** was isolated in 79% yield (73 mg).

**Catalytic Reduction under MW Conditions.** To an appropriate MW sealed tube containing the nitro compound **4a** (0.5 mmol) and 4 mL methanol were added 3 mmol of MeNHNH<sub>2</sub> and the cobalt(III) catalyst C1 (5% mol). The reaction mixture was irradiated, and according to the MW reactor readings (infrared-sensor), 100 °C and 2 bar were reached within the first minute. The irradiation continued at 50W, maintaining the reaction temperature at 100 °C and pressure 2 bar for a total time of 30 min. After that, the slurry was filtered

under reduced pressure through a short pad of silica gel to withhold the catalyst with the aid of ethyl acetate (~15 mL) for separating the catalyst from the reaction mixture. After solvent evaporation under a vacuum, the residue was purified with column chromatography using a gradient mixture of hexane–EtOAc (10:1 to 1:5), and the corresponding amine **4b** was isolated in 85% yield (39 mg).

#### Characterization and Spectroscopic Data of Compounds **1b–19b**.<sup>15a</sup>

**p-Toluidine (1b)**. The compound was isolated using a gradient mixture of hexane–EtOAc (10:1 to 1:4) as a brown solid. Mp: 41–43 °C (20 mg, 92% yield). <sup>1</sup>H NMR (500 MHz, CDCl<sub>3</sub>): 6.97 (d, *J* = 7.6 Hz, 2H), 6.62 (d, *J* = 7.6 Hz, 2H), 3.56 (br s, 2H), 2.25 (s, 3H). <sup>13</sup>C{H} NMR (125 MHz, CDCl<sub>3</sub>): 143.9, 129.9, 127.9, 115.4, 20.6.

**m-Toluidine (2b)**. The compound was isolated using a gradient mixture of hexane–EtOAc (10:1 to 1:4) as a light yellow liquid: 19 mg, 91% yield. <sup>1</sup>H NMR (500 MHz, CDCl<sub>3</sub>): 7.10 (t, *J* = 7.6 Hz, 1H), 6.65 (d, *J* = 7.5 Hz, 1H), 6.58–6.52 (m, 2H), 3.54 (s, 2H), 2.32 (s, 3H). <sup>13</sup>C{H} NMR (125 MHz, CDCl<sub>3</sub>): 146.3, 139.1, 129.2, 119.5, 116.0, 112.3, 21.5.<sup>3</sup>

**3,5-Dimethylaniline (3b)**. The compound was isolated using a gradient mixture of hexane–EtOAc (15:1 to 1:4) as a light-yellow liquid (22 mg, 91% yield). <sup>1</sup>H NMR (500 MHz, CDCl<sub>3</sub>): 6.43 (s, 1H), 6.34 (s, 2H), 3.48 (br s, 2H), 2.23 (s, 6H). <sup>13</sup>C{H} NMR (125 MHz, CDCl<sub>3</sub>): 146.5, 139.1, 120.6, 113.2, 21.4.<sup>32</sup>

**Aniline (4b)**. The compound was isolated using a gradient mixture of hexane–EtOAc (10:1 to 1:5) as a light-yellow liquid (16 mg, 88% yield). <sup>1</sup>H NMR (500 MHz, CDCl<sub>3</sub>): 7.16 (t, *J* = 7.8 Hz, 2H), 6.77 (t, *J* = 7.3 Hz, 1H), 6.70 (d, *J* = 7.8 Hz, 2H). <sup>13</sup>C{H} NMR (125 MHz, CDCl<sub>3</sub>): 129.3, 126.7, 118.7, 115.2.<sup>15a</sup>

**p-Anisidine (5b)**. The compound was isolated using a gradient mixture of hexane–EtOAc (10:1 to 1:7) as a brown solid. Mp: 57–59 °C (22 mg, 91% yield). <sup>1</sup>H NMR (500 MHz, CDCl<sub>3</sub>): 6.75 (d, *J* = 8.7 Hz, 2H), 6.65 (d, *J* = 8.7 Hz, 2H), 3.74 (s, 3H), 3.41 (br s, 2H). <sup>13</sup>C{H} NMR (125 MHz, CDCl<sub>3</sub>): 153.0, 139.9, 116.6, 114.9, 55.9.<sup>15a</sup>

**m-Anisidine (6b)**. The compound was isolated using a gradient mixture of hexane–EtOAc (10:1 to 1:5) as a light-yellow liquid (22 mg, 90% yield). <sup>1</sup>H NMR (500 MHz, CDCl<sub>3</sub>): 7.06 (t, *J* = 8.0 Hz, 1H), 6.33 (d, *J* = 8.0 Hz, 1H), 6.30 (d, *J* = 7.7 Hz, 1H), 6.25 (s, 1H), 3.76 (s, 3H), 3.68 (br s, 2H). <sup>13</sup>C{H} NMR (125 MHz, CDCl<sub>3</sub>): 160.9, 147.9, 130.2, 108.0, 104.1, 101.2, 55.2.<sup>15a</sup>

**4-(Benzyloxy)aniline (7b)**. The compound was isolated using a gradient mixture of hexane–EtOAc (15:1 to 1:5) as a white solid: Mp: 55–57 °C (35 mg, 89% yield). <sup>1</sup>H NMR (500 MHz, CDCl<sub>3</sub>): 7.53–7.32 (m, 4H), 7.34 (s, 1H), 6.84 (d, *J* = 8.6 Hz, 2H), 6.65 (d, *J* = 8.6 Hz, 2H), 5.00 (s, 2H), 3.50 (br s, 2H). <sup>13</sup>C{H} NMR (125 MHz, CDCl<sub>3</sub>): 152.1, 140.2, 137.6, 128.6, 127.9, 127.6, 116.5, 116.1, 70.8.<sup>15c</sup>

**p-Phenylenediamine (8b)**. The compound was isolated using a gradient mixture of hexane–EtOAc (10:1) as a yellow-brown liquid (20 mg, 92% yield). <sup>1</sup>H NMR (500 MHz, CDCl<sub>3</sub>): 6.56 (s, 4H), 3.25 (s, 4H). <sup>13</sup>C{H} NMR (125 MHz, CDCl<sub>3</sub>): 138.7, 116.8.<sup>15a</sup>

**p-Chloroaniline (9b)**. The compound was isolated using a gradient mixture of hexane–EtOAc (10:1 to 1:5) as a light-yellow solid. Mp: 69–72 °C (23 mg, 91% yield). <sup>1</sup>H NMR (500 MHz, CDCl<sub>3</sub>): 7.09 (d, *J* = 8.1 Hz, 2H), 6.60 (d, *J* = 8.1 Hz, 2H), 3.68 (s, 2H). <sup>13</sup>C{H} NMR (125 MHz, CDCl<sub>3</sub>): 145.1, 129.2, 123.3, 116.4.<sup>15a</sup>

**3-Amino-4-chloroanisole (10b)**. The compound was isolated using a gradient mixture of hexane–EtOAc (10:1 to 1:7) as a brown liquid–solid (28 mg, 90% yield). <sup>1</sup>H NMR (500 MHz, CDCl<sub>3</sub>): 7.11 (d, *J* = 8.6 Hz, 1H), 6.31 (s, 1H), 6.27 (d, *J* = 8.6 Hz, 1H), 4.01 (s, 2H), 3.73 (br s, 2H). <sup>13</sup>C{H} NMR (125 MHz, CDCl<sub>3</sub>): 159.5, 143.8, 129.9, 111.5, 105.0, 101.5, 55.5.<sup>15a</sup>

**p-Bromoanisole (11b)**. The compound was isolated using a gradient mixture of hexane–EtOAc (10:1 to 1:5) as a brown liquid (30 mg, 88% yield). <sup>1</sup>H NMR (500 MHz, CDCl<sub>3</sub>): 7.23 (d, *J* = 7.9 Hz, 2H), 6.56 (d, *J* = 7.9 Hz, 2H), 3.63 (br s, 2H). <sup>13</sup>C{H} NMR (125 MHz, CDCl<sub>3</sub>): 145.6, 132.1, 116.8, 110.3.<sup>15a</sup>

**Methyl 4-Aminobenzoate (12b)**. The compound was isolated using a gradient mixture of hexane–EtOAc (10:1 to 1:7) as a light-yellow solid. Mp: 110–112 °C (24 mg, 80% yield). <sup>1</sup>H NMR (500

MHz, CDCl<sub>3</sub>): 7.85 (d, *J* = 8.5 Hz, 2H), 6.63 (d, *J* = 8.5 Hz, 2H), 4.07 (s, 2H), 3.85 (s, 3H). <sup>13</sup>C{H} NMR (125 MHz, CDCl<sub>3</sub>): 167.3, 150.9, 131.7, 119.9, 113.9, 51.7.<sup>15a</sup>

**1-(4-Aminophenyl)ethenone (13b)**. The compound was isolated using a gradient mixture of hexane–EtOAc (10:1 to 1:8) as a yellow solid. Mp: 106–108 °C (28 mg, 89% yield). <sup>1</sup>H NMR (500 MHz, CDCl<sub>3</sub>): 7.81 (d, *J* = 8.2 Hz, 2H), 6.66 (d, *J* = 8.2 Hz, 2H), 4.31 (br s, 2H), 2.50 (s, 3H); <sup>13</sup>C{H} NMR (125 MHz, CDCl<sub>3</sub>): 196.6, 151.0, 130.9, 128.2, 114.0, 26.2.<sup>15a</sup>

**p-Aminobenzonitrile (14b)**. The compound was isolated using a gradient mixture of hexane–EtOAc (10:1) as a dark-yellow solid. Mp: 84–86 °C (20 mg, 85% yield). <sup>1</sup>H NMR (500 MHz, CDCl<sub>3</sub>): 7.39 (d, *J* = 8.5 Hz, 2H), 6.63 (d, *J* = 8.5 Hz, 2H), 4.20 (br s, 2H). <sup>13</sup>C{H} NMR (125 MHz, CDCl<sub>3</sub>): 153.0, 133.5, 121.0, 113.0, 95.5.<sup>11</sup>

**m-Aminobenzonitrile (15b)**. The compound was isolated using a gradient mixture of hexane–EtOAc (10:1) as a brown solid. Mp: 51–53 °C (23 mg, 89% yield). <sup>1</sup>H NMR (500 MHz, CDCl<sub>3</sub>): 7.21 (t, *J* = 7.9 Hz, 1H), 7.00 (d, *J* = 7.4 Hz, 1H), 6.89 (s, 1H), 6.86 (d, *J* = 7.9 Hz, 1H), 3.88 (br s, 2H). <sup>13</sup>C{H} NMR (125 MHz, CDCl<sub>3</sub>): 147.1, 130.2, 122.1, 119.3(2C), 117.5, 113.0.<sup>15a</sup>

**(3-Aminophenyl)sulfonamide (16b)**. The compound was isolated using a gradient mixture of hexane–EtOAc (5:1) as a yellow solid (31 mg, 91% yield). <sup>1</sup>H NMR (500 MHz, CD<sub>3</sub>OD): 7.24 (d, *J* = 7.8 Hz, 1H), 7.22 (s, 1H), 7.18 (d, *J* = 7.5 Hz, 1H), 6.89 (d, *J* = 7.8 Hz, 1H). <sup>13</sup>C{H} NMR (125 MHz, CD<sub>3</sub>OD): 149.8, 145.2, 130.6, 119.3, 115.5, 112.7.<sup>33</sup>

**6-Aminoisobenzofuran-1(3H)-one (17b)**. The compound was isolated using a gradient mixture of hexane–EtOAc (5:1) as a yellow solid. Mp: 178–180 °C (26 mg, 89% yield). <sup>1</sup>H NMR (500 MHz, CD<sub>3</sub>OD): 7.29 (d, *J* = 7.6 Hz, 1H), 7.11–7.04 (m, 2H), 5.23 (s, 2H). <sup>13</sup>C{H} NMR (125 MHz, CD<sub>3</sub>OD): 174.3, 150.7, 137.3, 127.3, 123.8, 123.2, 109.7, 71.3.<sup>15c</sup>

**1H-Benzo[d]imidazol-5-amine (18b)**. The compound was isolated using a gradient mixture of hexane–EtOAc (5:1) as a brown solid. Mp: 107–110 °C (24 mg, 86% yield). <sup>1</sup>H NMR (500 MHz, CD<sub>3</sub>OD): 7.99 (s, 1H), 7.36 (d, *J* = 8.6 Hz, 1H), 6.92 (s, 1H), 6.77 (d, *J* = 8.6 Hz, 1H). <sup>13</sup>C{H} NMR (125 MHz, CD<sub>3</sub>OD): 144.9, 140.9, 139.7, 117.2, 114.8(2C), 100.4.<sup>34</sup>

**1H-Indazol-6-amine (19b)**. The compound was isolated using a gradient mixture of hexane–EtOAc (5:1) as a yellow liquid (23 mg, 85% yield). <sup>1</sup>H NMR (500 MHz, CD<sub>3</sub>OD): 7.78 (s, 1H), 7.45 (d, *J* = 8.6 Hz, 1H), 6.69 (d, *J* = 1.8 Hz, 1H), 6.63 (dd, *J* = 8.6, 1.8 Hz, 1H). <sup>13</sup>C{H} NMR (125 MHz, CD<sub>3</sub>OD): 147.3, 142.1, 133.2, 120.7, 116.5, 113.2, 91.9.<sup>15a</sup>

## ■ ASSOCIATED CONTENT

### Supporting Information

The Supporting Information is available free of charge at <https://pubs.acs.org/doi/10.1021/acs.joc.0c02814>.

Detailed experimental procedures, compound characterization data, and mechanistic analysis experiments (PDF)

### Accession Codes

CCDC 1995930 contains the supplementary crystallographic data for this paper. These data can be obtained free of charge via [www.ccdc.cam.ac.uk/data\\_request/cif](http://www.ccdc.cam.ac.uk/data_request/cif), or by emailing [data\\_request@ccdc.cam.ac.uk](mailto:data_request@ccdc.cam.ac.uk), or by contacting The Cambridge Crystallographic Data Centre, 12 Union Road, Cambridge CB2 1EZ, UK; fax: +44 1223 336033.

## ■ AUTHOR INFORMATION

### Corresponding Authors

Panagiotis A. Angaridis – Department of Chemistry, Aristotle University of Thessaloniki, Thessaloniki 54124, Greece; Email: [panosangaridis@chem.auth.gr](mailto:panosangaridis@chem.auth.gr)

Ioannis N. Lykakis – Department of Chemistry, Aristotle University of Thessaloniki, Thessaloniki 54124, Greece; [orcid.org/0000-0001-8165-5604](https://orcid.org/0000-0001-8165-5604); Email: [lykakis@chem.auth.gr](mailto:lykakis@chem.auth.gr)

## Authors

Dimitris I. Ioannou – Department of Chemistry, Aristotle University of Thessaloniki, Thessaloniki 54124, Greece  
Dimitra K. Gioftsidou – Department of Chemistry, Aristotle University of Thessaloniki, Thessaloniki 54124, Greece  
Vasiliki E. Tsina – Department of Chemistry, Aristotle University of Thessaloniki, Thessaloniki 54124, Greece  
Michael G. Kallitsakis – Department of Chemistry, Aristotle University of Thessaloniki, Thessaloniki 54124, Greece  
Antonios G. Hatzidimitriou – Department of Chemistry, Aristotle University of Thessaloniki, Thessaloniki 54124, Greece  
Michael A. Terzidis – Department of Nutritional Sciences and Dietetics, International Hellenic University, Thessaloniki 57400, Greece

Complete contact information is available at:  
<https://pubs.acs.org/10.1021/acs.joc.0c02814>

## Notes

The authors declare no competing financial interest.

## ACKNOWLEDGMENTS

The authors kindly acknowledge financial support from the Hellenic Foundation for Research and Innovation (HFRI) and the General Secretariat for Research and Technology (GSRT) under grant agreement no. [776] “PhotoDaLu” (KA97507). We acknowledge the support of this work by the project “An Open-Access Research Infrastructure of Chemical Biology and Target-Based Screening Technologies for Human and Animal Health, Agriculture and the Environment (OPENSREEN-GR)” (MIS 5002691), which is implemented under the Action “Reinforcement of the Research and Innovation Infrastructure”, funded by the Operational Programme “Competitiveness, Entrepreneurship and Innovation” (NSRF 2014-2020) and cofinanced by Greece and the European Union (KA94150). I.N.L. kindly acknowledges the “Empeirikeion Foundation” for financial support. The Center of Interdisciplinary Research and Innovation of Aristotle University of Thessaloniki (CIRI-AUTH) is also acknowledged for providing access to the Large Research Infrastructure and Instrumentation of the NMR Laboratory in the Chemical Engineering Department, AUTH, as well as the Chemistry Department, AUTH, for providing access to the Large Research Instrumentation single-crystal XRD Unit. We thank Dr. C. Gabriel of the HERACLES Research Center, KEDEK, Laboratory of Environmental Engineering (EnvE-Lab), Department of Chemical Engineering, AUTH, Greece, for using the LC-TOF mass spectrometer and performing the HRMS experiments.

## REFERENCES

(1) (a) Blaser, H.-U.; Steiner, H.; Studer, M. Selective Catalytic Hydrogenation of Functionalized Nitroarenes: An Update. *ChemCatChem* **2009**, *1*, 210–221. (b) Serna, P.; Corma, A. Transforming Nano Metal Nonselective Particulates into Chemoselective Catalysts for Hydrogenation of Substituted Nitrobenzenes. *ACS Catal.* **2015**, *5*, 7114–7121. (c) Orlandi, M.; Brenna, D.; Harms, R.; Jost, S.; Benaglia, M. Recent Developments in the Reduction of Aromatic and

Aliphatic Nitro Compounds to Amines. *Org. Process Res. Dev.* **2018**, *22*, 430–445. (d) Song, J.; Huang, Z.-F.; Pan, L.; Li, K.; Zhang, X.; Wang, L.; Zou, J.-J. Review on Selective Hydrogenation of Nitroarene by Catalytic, Photocatalytic and Electrocatalytic Reactions. *Appl. Catal., B* **2018**, *227*, 386–408. (e) Formenti, D.; Ferretti, F.; Scharnagl, F. K.; Beller, M. Reduction of Nitro Compounds Using 3d-Non-Noble Metal Catalysts. *Chem. Rev.* **2019**, *119*, 2611–2680.

(2) (a) Pellissier, H.; Clavier, H. Enantioselective Cobalt-Catalyzed Transformations. *Chem. Rev.* **2014**, *114*, 2775–2823. (b) Renaud, J.-L.; Gaillard, S. Recent Advances in Iron- and Cobalt-Complex-Catalyzed Tandem/Consecutive Processes Involving Hydrogenation. *Synthesis* **2016**, *48*, 3659–3683. (c) Liu, W.; Sahoo, B.; Junge, K.; Beller, M. Cobalt Complexes as an Emerging Class of Catalysts for Homogeneous Hydrogenations. *Acc. Chem. Res.* **2018**, *51*, 1858–1869.

(3) Vernekar, A. A.; Patil, S.; Bhat, C.; Tilve, S. G. Magnetically Recoverable Catalytic Co–Co<sub>2</sub>B Nanocomposites for the Chemoselective Reduction of Aromatic Nitro Compounds. *RSC Adv.* **2013**, *3*, 13243–13250.

(4) Zhao, Z.; Yang, H.; Li, Y.; Guo, X. Cobalt-Modified Molybdenum Carbide as an Efficient Catalyst for Chemoselective Reduction of Aromatic Nitro Compounds. *Green Chem.* **2014**, *16*, 1274–1281.

(5) Zhang, J.; Lu, G.; Cai, C. Chemoselective Transfer Hydrogenation of Nitroarenes by Highly Dispersed Ni-Co BMNPs. *Catal. Commun.* **2016**, *84*, 25–29.

(6) Yuan, M.; Zhang, H.; Yang, C.; Wang, F.; Dong, Z. Co-MOF-Derived Hierarchical Mesoporous Yolk-shell-structured Nanoreactor for the Catalytic Reduction of Nitroarenes with Hydrazine Hydrate. *ChemCatChem* **2019**, *11*, 3327–3338.

(7) Reddy, P. L.; Tripathi, M.; Arundhati, R.; Rawat, D. S. Chemoselective Hydrazine-mediated Transfer Hydrogenation of Nitroarenes by Co<sub>3</sub>O<sub>4</sub> Nanoparticles Immobilized on an Al/Si-mixed Oxide Support. *Chem. - Asian J.* **2017**, *12*, 785–791.

(8) Albadi, J.; Samimi, H. A.; Jalali, M. Chemoselective Reduction of Nitroarenes with Hydrazine over a Highly Active Alumina-Supported Cobalt Nanocatalyst. *Acta Chim. Slov.* **2019**, *66*, 740–744.

(9) Sharma, U.; Kumar, P.; Kumar, N.; Kumar, V.; Singh, B. Highly Chemo- and Regioselective Reduction of Aromatic Nitro Compounds Catalyzed by Recyclable Copper(II) as well as Cobalt(II) Phthalocyanines. *Adv. Synth. Catal.* **2010**, *352*, 1834–1840.

(10) Chao, C.-G.; Bergbreiter, D. E. Highly Organic Phase Soluble Polyisobutylene-Bound Cobalt Phthalocyanines as Recyclable Catalysts for Nitroarene Reduction. *Catal. Commun.* **2016**, *77*, 89–93.

(11) Srivastava, S.; Dagur, M. S.; Ali, A.; Gupta, R. Trinuclear {Co<sup>2+</sup>–M<sup>3+</sup>–Co<sup>2+</sup>} Complexes Catalyze Reduction of Nitro Compounds. *Dalton Trans* **2015**, *44*, 17453–17461.

(12) (a) Yadav, S.; Kumar, S.; Gupta, R. Cobalt Complexes of Pyrrolecarboxamide Ligands as Catalysts in Nitro Reduction Reactions: Influence of Electronic Substituents on Catalysis and Mechanistic Insights. *Inorg. Chem. Front.* **2017**, *4*, 324–335. (b) Kumar, S.; Gupta, R. Cobalt Complexes Catalyze Reduction of Nitro Compounds: Mechanistic Studies. *ChemistrySelect* **2017**, *2*, 8197–8206.

(13) Rai, R. K.; Mahata, A.; Mukhopadhyay, S.; Gupta, S.; Li, P.-Z.; Nguyen, K. T.; Zhao, Y.; Pathak, B.; Singh, S. K. Room-Temperature Chemoselective Reduction of Nitro Groups Using Non-noble Metal Nanocatalysts in Water. *Inorg. Chem.* **2014**, *53*, 2904–2909.

(14) Amanchi, S. R.; Ashok Kumar, K. V.; Lakshminarayana, B.; Satyanarayana, G.; Subrahmanyam, Ch. Photocatalytic Hydrogenation of Nitroarenes: Supporting Effect of CoO<sub>x</sub> on TiO<sub>2</sub> Nanoparticles. *New J. Chem.* **2019**, *43*, 748–754.

(15) (a) Gkizis, P. L.; Stratakis, M.; Lykakis, I. N. Catalytic Activation of Hydrazine Hydrate by Gold Nanoparticles: Chemoselective Reduction of Nitro Compounds into Amines. *Catal. Commun.* **2013**, *36*, 48–51. (b) Fountoulaki, S.; Daikopoulou, V.; Gkizis, P. L.; Tamiolakis, I.; Armatas, G. S.; Lykakis, I. N. Mechanistic Studies of the Reduction of Nitroarenes by NaBH<sub>4</sub> or Hydrosilanes Catalyzed by Supported Gold Nanoparticles. *ACS Catal.* **2014**, *4*,

- 3504–3511. (c) Vasilikogiannaki, E.; Gryparis, C.; Kotzabasaki, V.; Lykakis, I. N.; Stratakis, M. Activation of Ammonia-Borane Complex by Gold Nanoparticles: Facile Reduction of Nitroarenes into Anilines and Nitroalkanes into Hydroxylamines. *Adv. Synth. Catal.* **2013**, *355*, 907–911. (d) Papadas, I. T.; Fountoulaki, S.; Lykakis, I. N.; Armatas, G. S. Controllable Synthesis of Mesoporous Iron Oxide Nanoparticle Assemblies for Chemoselective Catalytic Reduction of Nitroarenes. *Chem. - Eur. J.* **2016**, *22*, 4600–4607. (e) Charistoudi, E.; Kallitsakis, M. G.; Charisteidis, I.; Triantafyllidis, K. S.; Lykakis, I. N. Selective Reduction of Azines to Benzyl Hydrazones with Sodium Borohydride Catalyzed by Mesoporous Silica-Supported Silver Nanoparticles: A Catalytic Route towards Pyrazole Synthesis. *Adv. Synth. Catal.* **2017**, *359*, 2949–2960. (f) Tzani, M. A.; Kallitsakis, M. G.; Symeonidis, T. S.; Lykakis, I. N. Alumina Supported Gold Nanoparticles as a Bifunctional Catalyst for the Synthesis of 2-Amino-3-arylimidazo[1,2-a]pyridines. *ACS Omega* **2018**, *3*, 17947–17956. (g) Kallitsakis, M. G.; Ioannou, D. I.; Terzidis, M. A.; Kostakis, G. E.; Lykakis, I. N. Selective photoinduced reduction of nitroarenes to N-arylhydroxylamines. *Org. Lett.* **2020**, *22*, 4339–4343.
- (16) (a) Raper, E. S. Complexes of Heterocyclic Thionates. Part 1. Complexes of Monodentate and Chelating Ligands. *Coord. Chem. Rev.* **1996**, *153*, 199–255. (b) Raper, E. S. Complexes of Heterocyclic Thionates Part 2: Complexes of Bridging Ligands. *Coord. Chem. Rev.* **1997**, *165*, 475–567. (c) Das, A.; Han, Z.; Brennessel, W. W.; Holland, P. L.; Eisenberg, R. Nickel Complexes for Robust Light-Driven and Electrocatalytic Hydrogen Production from Water. *ACS Catal.* **2015**, *5*, 1397–1406.
- (17) A similar crystal structure to  $\text{C1} \cdot 0.16\text{CH}_2\text{Cl}_2$ , which contains **C1** in its unsolvated form that belongs to a different space group (obtained by electrochemical synthesis), was reported in the past. Rodríguez, A.; García-Vázquez, J. A.; Romero, J.; Sousa-Pedrares, A.; Sousa, A.; Castro, J. Z. Electrochemical Synthesis and Characterization of Cobalt(II), Cobalt(III), and Nickel(II) Complexes with Pyrimidine-2-thionato Ligands. *Z. Anorg. Allg. Chem.* **2007**, *633*, 763–770.
- (18) (a) Rosenfield, S. G.; Berends, H. P.; Gelmini, L.; Stephan, D. W.; Mascharak, P. K. New Octahedral Thiolato Complexes of Divalent Nickel: Syntheses, Structures, and Properties of  $(\text{Et}_4\text{N})[\text{Ni}(\text{SC}_5\text{H}_4\text{N})_3]$  and  $(\text{Ph}_4\text{P})[\text{Ni}(\text{SC}_4\text{H}_3\text{N}_2)_3] \cdot \text{CH}_3\text{CN}$ . *Inorg. Chem.* **1987**, *26*, 2792–2797. (b) Deeming, A. J.; Hardcastle, K. I.; Meah, M. N.; Bates, P. A.; Dawes, H. M.; Hursthouse, M. B. Rhodium(III) Complexes with Pyridine-2-thiol (pySH) and Pyridine-2-thiolato (pyS) as the only Ligands: Crystal Structures of *mer*- $[\text{Rh}(\text{pyS})_3]$ ,  $[\text{Rh}(\text{pyS})_2(\text{pySH})_2]\text{Cl} \cdot 0.5\text{H}_2\text{O}$ , and  $[\text{Rh}(\text{pyS})_3(\text{pySH})]$ . *J. Chem. Soc., Dalton Trans.* **1988**, *1*, 227–233. (c) Fielding, C.; Parsons, S.; Wimpenny, R. E. P. *fac*-Tris(6-methyl-2-mercaptopyridinato)cobalt(III) at 150K. *Acta Crystallogr., Sect. C: Cryst. Struct. Commun.* **1997**, *53*, 174–176. (d) Seth, S. Tris(4,6-dimethylpyrimidine-2-thiolato-N,S)cobalt(III) Monohydrate: a Complex with Three Stable Four-membered N,S-chelate Rings. *Acta Crystallogr., Sect. C: Cryst. Struct. Commun.* **1994**, *50*, 1196–1199.
- (19) Han, Z.; Shen, L.; Brennessel, W. W.; Holland, P. L.; Eisenberg, R. Nickel Pyridylthiolate Complexes as Catalysts for the Light-Driven Production of Hydrogen from Aqueous Solutions in Noble-Metal-Free Systems. *J. Am. Chem. Soc.* **2013**, *135*, 14659–14669.
- (20) King, D. M.; Bard, A. J. The Electrochemistry of the Methylhydrazines. *J. Am. Chem. Soc.* **1965**, *87*, 419–423.
- (21) Sandford, C.; Edwards, M. A.; Klunder, K. J.; Hickey, D. P.; Li, M.; Barman, K.; Sigman, M. S.; White, H. S.; Minter, S. D. A synthetic chemist's guide to electroanalytical tools for studying reaction mechanisms. *Chem. Sci.* **2019**, *10*, 6404–6422.
- (22) Ai, W.; Zhong, R.; Liu, X.; Liu, Q. Hydride Transfer Reactions Catalyzed by Cobalt Complexes. *Chem. Rev.* **2019**, *119*, 2876–2953.
- (23) (a) Bauer, J. O.; Leitus, G.; David, Y. B.; Milstein, D. Direct Synthesis of Symmetrical Azines from Alcohols and Hydrazine Catalyzed by a Ruthenium Pincer Complex: Effect of Hydrogen Bonding. *ACS Catal.* **2016**, *6*, 8415–8419. (b) Bezdek, M. J.; Guo, S.; Chirik, P. J. Coordination-induced weakening of ammonia, water, and hydrazine X–H bonds in a molybdenum complex. *Science* **2016**, *354*, 730–733.
- (24) Albertin, G.; Antonutti, S.; Bortoluzzi, M.; Botter, A.; Castro, J. Pentamethylcyclopentadienyl Half-Sandwich Diazoalkane Complexes of Ruthenium: Preparation and Reactivity. *Inorg. Chem.* **2016**, *55*, 5592–5602.
- (25) Lambert, C. E.; Shank, R. C. Role of Formaldehyde Hydrazone and Catalase in Hydrazine-induced Methylation of DNA Guanine. *Carcinogenesis* **1988**, *9*, 65–70.
- (26) Field, L. D.; Li, H. L.; Dalgarno, S. J.; McIntosh, R. D. Base-Induced Dehydrogenation of Ruthenium Hydrazine Complexes. *Inorg. Chem.* **2013**, *52*, 1570–1583.
- (27) Haber, F. Z. *Elektrochem. Angew. Phys. Chem.* **1898**, *4*, 410–413.
- (28) (a) Corma, A.; Concepcion, P.; Serna, P. A Different Reaction Pathway for the Reduction of Aromatic Nitro Compounds on Gold Catalysts. *Angew. Chem., Int. Ed.* **2007**, *46*, 7266–7269. (b) Gelder, E. A.; Jackson, S. D.; Lok, C. M. The Hydrogenation of Nitrobenzene to Aniline: a New Mechanism. *Chem. Commun.* **2005**, 522–524.
- (29) Apex2, Version 2 User Manual, M86-E01078; Bruker Analytical X-ray Systems, Inc: Madison, WI, 2006
- (30) Betteridge, P. W.; Carruthers, J. R.; Cooper, R. I.; Prout, K.; Watkin, D. J. Crystals Version 12: Software for Guided Crystal Structure Analysis. *J. Appl. Crystallogr.* **2003**, *36*, 1487.
- (31) Macrae, C. F.; Edgington, P. R.; McCabe, P.; Pidcock, E.; Shields, G. P.; Taylor, R.; Towler, M.; van de Streek, J. Mercury: Visualization and Analysis of Crystal Structures. *J. Appl. Crystallogr.* **2006**, *39*, 453–457.
- (32) Li, Z.; Yu, H.; Bolm, C. Dibenzothiophene Sulfoximine as an  $\text{NH}_3$  Surrogate in the Synthesis of Primary Amines by Copper-Catalyzed C-X and C-H Bond Amination. *Angew. Chem., Int. Ed.* **2017**, *56*, 9532–9535.
- (33) Buděšínský, M.; Johnels, D.; Edlund, U.; Exner, O. Carbon-13 Substituent-induced Chemical Shifts in Benzene Derivatives: Substituted Anilines. *Collect. Czech. Chem. Commun.* **1991**, *56*, 368–385.
- (34) Karuvalam, Ranjith. P.; Siji, M.; Divia, N.; Haridas, Karickal. R. Tetra Butyl Ammonium Chloride Catalyzed Synthesis of Substituted Benzimidazoles under Microwave Conditions. *J. Korean Chem. Soc.* **2010**, *54*, 589–593.